International Journal of Hybrid Information Technology
Vol. 9, No. 5 (2016), pp. 407-418
http://dx.doi.org/10.14257/ijhit.2016.9.5.35

Infrared and Visible Image Fusion Method Based On Three Stages of Discrete Wavelet Transform

Lingchao Zhan[1,2] and Yi Zhuang[1]

[1] *College of Computer Science and Technology, Nanjing University of Aeronautics and Astronautics, Nanjing, China*
[2] *Nanhang Jincheng College, Nanjing, China*
lingchao_zhan@163.com

Abstract

For infrared images, the performance of texture details in the target scene is not good, and for visible images, the performance is constrained by illumination and environment. An image fusion method is proposed here, its characteristic is getting three different discrete wavelet fusion methods together. The method has three stages, in the first two stages, the infrared and visible images are fused using different wavelet fusion rules, the two fusion results from the first and the second stage are fused again using another wavelet fusion rule, and then we get the final fusion result. The result proves that, compared with the similar research methods, the proposed method can ensure the quality and enhance the spatial detail of the fused image.

Keywords*: image fusion; infrared image; visible0 image; discrete wavelet transform*

1. Introduction

Image fusion is the method to fuse two or more images into a single image, this fused image should include more information. In recent years, image fusion technology is applied in many fields, such as remote sensing, medical image processing, robot vision and digital camera application.

Infrared and visible image fusion method is one of the image fusion methods. The infrared image is the result of the infrared thermal imaging sensors detecting the outside temperature difference. It can work all day and not easily affected by the environment, but the performance of the image texture details is not good. The visible image is suitable for human visual characteristics, but it is constrained by lighting and environmental conditions. For these characteristics of the two kinds of images, we fuse them together. Not only have the promise of the quality, but also make the image clearer. It can improve the image resolution and enhance the details. It is convenient for human identification.

Image fusion can be divided into the pixel level fusion, feature level fusion and decision level fusion. The pixel level fusion is the fusion of the source image data. It directly fuses the multi source images of the same scene together. The feature level image fusion has two steps. The pretreatment and feature extraction of the source images is the first step, the second step is the fusion of the various features. The decision level fusion is a kind of high level data fusion. First, for the multiple source images, each feature of the same target is classified and judged. Then the independent decisions of each source images will be fused together. Finally, the joint decision will be obtained. At present, most of the fusion methods are pixel level fusion [1]. Commonly used methods include PCA [6], the Pyramid transform [7] [8] ,wavelet transform[2]-[4],[9]-[19]. PCA is a method of selecting optimal pixel weight. The disadvantage is it cannot prominent spectral characteristics, so it is not suitable for

ISSN: 1738-9968 IJHIT

the weak correlation of image fusion. The Pyramid decomposition aims to decompose images into different spatial frequency. Using the characteristics of the decomposition of the tower structure has different decomposition layers in different spatial resolution, it adopts different fusion operators. Finally, the characteristics and details which are from different images will be fused together. But it leads to bad fusion result because of the correlation between the layers.

The wavelet transform has good performance in preserving image information. Different results can be obtained through different fusion rules. For the result of the simple single wavelet transform fusion is not good, this paper proposes a method based on three stages of wavelet transform. In the first and the second stage, the infrared and visible images are fused using different fusion rules. In the third stage, the two results of the first and second stage are fused again using another fusion rule. We compare our results with the simplest wavelet fusion method AVE_MAX [3], the first and the second stage of our method. We use four objective evaluation standards, they are mean, standard deviation, entropy and average gradient. The results show that our method has a good effect, our fusion result is clearer, especially the high growth of the average gradient.

2. Related Research

2.1. Related Research Based on Wavelet Transform

Wavelet transform was first proposed by the French scientist Morlet and Grossman in the early 1980s [14]. With the rise of wavelet theory, especially after scientist Mallat S G proposed the fast wavelet transform algorithm [9], wavelet transform has been widely applied in the field of image processing. Now it has been a typical image fusion tool. Compared with the pyramid transform, decomposition coefficients between different resolutions are not relevant.

In the early 1990s, Li H *et al* [11] and Chipman LJ et al [12] first proposed the concept of image fusion based on wavelet analysis. With the continuous development of wavelet theory and the requirements of improving the image fusion, KingsburyN proposed dual tree complex wavelet transform has better direction selectivity and approximate translation invariance[17], Yifeng Niu *et al*[16] proposed fusion method of combining wavelet transform with other methods. In addition, man [18] [19]y scholars have proposed various image fusion methods using wavelet transform [. In this paper, fusion method based on three stages of wavelet transform is proposed for the fusion of visible and infrared images.

2.2. Fusion Method Based on Wavelet Transform

For the inspiration of the tower algorithm for image decomposition and reconstruction, Mallat proposed wavelet decomposition and reconstruction algorithm based on multi-resolution theory that is the Mallat fast algorithm. If an image is decomposed using wavelet transform and the level is J, the image will be decomposed into one low frequency component and 3J high frequency components. Set scaling function and filter coefficient matrix H and G, respectively. The image wavelet decomposition formulas are shown in (1).

$$\begin{cases} C_{j+1} = HC_jH' \\ D_{j+1}^h = GC_jH' \\ D_{j+1}^v = HC_jG' \\ D_{j+1}^d = GC_jG' \end{cases} \qquad j = 0,1,...,J-1 \tag{1}$$

The corresponding reconstruction formula is shown in (2).

$$C_j = H'C_{j+1}H + G'D_{j+1}^h H + H'D_{j+1}^v G + G'D_{j+1}^d G \qquad j = J-1,...,1,0 \qquad (2)$$

For the image C_j, the low frequency component is C_{j+1}, the high frequency component in the horizontal direction is D_{j+1}^h, the high frequency component in the vertical direction is D_{j+1}^v, the high frequency component in the diagonal direction is D_{j+1}^d. H' and G' are the conjugate transpose matrices of H and G, respectively.

3. IVFTWT Method

3.1. The Motivation of the IVFTWT Method

Infrared sensors identify target by detecting differences in thermal radiation between target and background. The infrared image can reflect the existing characteristics of the target, but the gray value of the image is determined by the temperature difference between the target and background. It cannot reflect the real scene and the exact location of the target, so its visual effect is not good and cannot distinguish image details. Visible sensors are sensitive to the brightness changes in the scenes, the obtained image can have a high resolution. But in the case of sheltered or poor lighting, the visible image will have low contrast. So each image used alone can have advantages and disadvantages.

For the characteristics of the infrared and visible images, a fusion method named IVFTWT is proposed in this paper. This method is Infrared and Visible Image Fusion Method Based on Three Stages of Discrete Wavelet Transform.

3.2. The Design of the IVFTWT Rules

The more levels of the wavelet transform, the more details in the fusion result. But with the increase of decomposition levels, the image structural information loss will become larger, this information will not be recovered in the inverse wavelet transform. So the wavelet decomposition level cannot be too large, generally between 2 to 5. It has proved by experiments and we consider the running time, this paper choose 2 as the decomposition levels.

Definition 1: The two images to be fused are image A and image B. They are decomposed using discrete wavelet transform. After the decomposition, the low frequency component of image A is $L_A(x,y)$ and the low frequency component of image B is $L_B(x,y)$. The high frequency component are represented by $H_A^{h1}(x,y)$, $H_A^{v1}(x,y)$, $H_A^{d1}(x,y)$, $H_A^{h2}(x,y)$, $H_A^{v2}(x,y)$, $H_A^{d2}(x,y)$, $H_B^{h1}(x,y)$, $H_B^{v1}(x,y)$, $H_B^{d1}(x,y)$, $H_B^{h2}(x,y)$, $H_B^{v2}(x,y)$, $H_B^{d2}(x,y)$, they are the horizontal, vertical and diagonal high frequency components of the first and the second level, respectively.

The DWT decomposition diagrams of image A and B are shown in figure 1.

(a). decomposition diagram of image A (b)decomposition diagram of image B

Figure1. The DWT Decomposition Diagrams of Image A and B

The low and high frequency components of the image A and B will be fused using different fusion rules. Our rules are as follows:

(1)The first stage: For the low frequency component, the coefficient is determined by the regional energy. If the regional energy of image A is greater than that of image B, the low frequency coefficients of image A will be selected as the fusion result in this region, otherwise, the low frequency coefficients of image B will be selected. For the high frequency component, the result is to select the maximum value of the coefficients. If the high frequency coefficient value of image A is greater than that of image B, the high frequency coefficient of image A will be selected, else the coefficient of image B will be selected. The inverse wavelet transform will be taken to the resulting low and high frequency coefficients, we will get the result of the first stage.

(2)The second stage: For the low frequency component, the regional energy will first be calculated, the formula is the same as that of the first stage. The correlation of the low frequency coefficients is calculated according to the energy value. The low frequency coefficients will be determined by the energy value and the correlation value, the specific description is in Section 3.3. For the high frequency component, the result is to select the maximum absolute value of the coefficients. If the absolute high frequency coefficient value of image A is greater than that of image B, the high frequency coefficient of image A will be selected, else the coefficient of image B will be selected. The inverse wavelet transform will be taken to the resulting low and high frequency coefficients, we will get the result of the second stage.

(3) The third stage: The results of the first and the second stage will be fused together. For the low frequency component, the result is still determined by calculating the regional energy of the low frequency coefficients, the energy formula is slightly different here. If the regional energy of image A is greater than that of image B, the low frequency coefficients of image A will be selected as the fusion result in this region, otherwise, the low frequency coefficients of image B will be selected. For the high frequency component, the result is determined by the regional standard deviation. If the regional standard deviation of image A is greater than that of image B, the high frequency coefficients of image A will be selected as the fusion result in this region, otherwise, the high frequency coefficients of image B will be selected. The inverse wavelet transform will be taken to the resulting low and high frequency coefficients, we will get the final result.

3.3. The Diagram of IVFTWT Method

The two images to be fused are image A and B, the diagram of IVFTWT method is shown in figure 2.

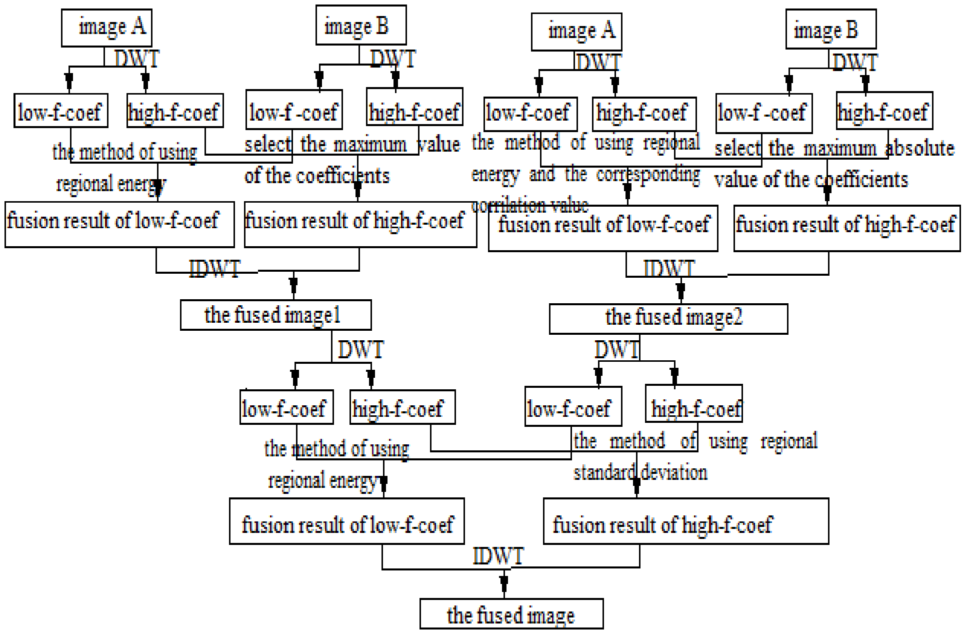

Figure 2.The Diagram of IVFTWT Method

3.4. The Description of IVFTWT Method

The IVFTWT method has three stages. In the first and the second stage, the two images to be fused are image A and image B, the two images are fused using different fusion rules. In the third stage, the two images to be fused are the results from the first and the second stage, the two images are fused using another fusion rule. “db2” is selected as the wavelet basis.

The IVFTWT method is described as follows:

(1)The first stage:

a. the calculation method of the low frequency component

The low frequency components of the two images are divided into discrete 3×3 regions. (we have tried the dimensions of 3×3 and 5×5, experiments show that the 3×3 is better. The following are all divided into discrete 3×3 regions.) Then we calculate each regional energy. Suppose E_A and **Error! Reference source not found.** represent the regional energy of the image A and image B. The energy formulae are shown in (3) and (4) [15] [16].

$$E_A = \sum_{x=1}^{3}\sum_{y=1}^{3} L_A^2(x,y) \qquad (3)$$

$$E_B = \sum_{x=1}^{3}\sum_{y=1}^{3} L_B^2(x,y) \qquad (4)$$

The low frequency component of the fused image is determined by the value of the regional energy. If the regional energy of image A is greater than that of image B, the low frequency component of image A will be selected as the fusion result, else the low frequency component of image B will be selected. Suppose the low frequency component of the fused image is $L_1(x,y)$, the fusion formula of the low frequency component is shown in (5) [16].

$$L_1(x,y) = \begin{cases} L_A(x,y) & E_A \ge E_B \\ L_B(x,y) & E_A < E_B \end{cases} \qquad (5)$$

b. the calculation method of the high frequency components

The maximum value of the high frequency component will be selected. Suppose $H_1^{h1}(x,y)$, $H_1^{v1}(x,y)$, $H_1^{d1}(x,y)$, $H_1^{h2}(x,y)$, $H_1^{v2}(x,y)$, $H_1^{d2}(x,y)$ represent the first and second level fusion results of the horizontal, vertical and diagonal high frequency components, respectively. The fusion formulae of the high frequency components are shown in (6)-(11) [3].

$$H_1^{h1}(x,y) = \max(H_A^{h1}(x,y), H_B^{h1}(x,y)) \tag{6}$$

$$H_1^{v1}(x,y) = \max(H_A^{v1}(x,y), H_B^{v1}(x,y)) \tag{7}$$

$$H_1^{d1}(x,y) = \max(H_A^{d1}(x,y), H_B^{d1}(x,y)) \tag{8}$$

$$H_1^{h2}(x,y) = \max(H_A^{h2}(x,y), H_B^{h2}(x,y)) \tag{9}$$

$$H_1^{v2}(x,y) = \max(H_A^{v2}(x,y), H_B^{v2}(x,y)) \tag{10}$$

$$H_1^{d2}(x,y) = \max(H_A^{d2}(x,y), H_B^{d2}(x,y)) \tag{11}$$

The inverse wavelet transform will be taken to the resulting low and high frequency coefficients, we will get the fusion result of the first stage.

(2)The second stage:

a. the calculation method of the low frequency component

We choose the method in [2]. We divide the low frequency components of the two images into discrete 3×3 regions, then the regional energy will be calculated, the energy formulae are (3) and (4). It is the same as the first step.

The correlation of the low frequency coefficients is calculated according to the energy value. The correlation is the relationship between the corresponding regions of the low frequency coefficients. The formula for calculating the correlation is shown in (12) [2].

$$M = \frac{2\times\sum_{x=1}^{3}\sum_{y=1}^{3} L_A(x,y)\times L_B(x,y)}{m\times n\times(E_A+E_B)} \tag{12}$$

$m=n=3$, E_A and E_B are the corresponding regional energies of the low frequency components.

Suppose the low frequency component of the fused image is $L_2(x,y)$ **Error! Reference source not found.**. The value of M in (12) is in the range of 0~1, we choose 0.7 as the threshold of M. If $M<0.7$, the low frequency component will be obtained by (13)[2], else the low frequency component will be obtained by (14)[2].

$$L_2(x,y) = \begin{cases} L_A(x,y) & E_A \ge E_B \\ L_B(x,y) & E_A < E_B \end{cases} \tag{13}$$

$$L_2(x,y) = \begin{cases} \alpha\times L_A(x,y) + (1-\alpha)\times L_B(x,y) & E_A \ge E_B \\ (1-\alpha)\times L_A(x,y) + \alpha\times L_B(x,y) & E_A < E_B \end{cases} \tag{14}$$

$$\alpha = \frac{1}{2} + \frac{1}{2}\left[\frac{1-M}{1-T}\right]$$

b. the calculation method of the high frequency components

The fusion result is to select the maximum absolute value of the high frequency coefficients.

Suppose $H_2^{h1}(x,y)$, $H_2^{v1}(x,y)$, $H_2^{d1}(x,y)$, $H_2^{h2}(x,y)$, $H_2^{v2}(x,y)$, $H_2^{d2}(x,y)$ represent the first and second level fusion results of the horizontal, vertical and diagonal high frequency components, respectively. The fusion formulae of the high frequency components are shown in (15) ~(20)[14].

$$H_2^{h1}(x,y) = \begin{cases} H_A^{h1}(x,y) & \left|H_A^{h1}(x,y)\right| \geq \left|H_B^{h1}(x,y)\right| \\ H_B^{h1}(x,y) & \left|H_A^{h1}(x,y)\right| < \left|H_B^{h1}(x,y)\right| \end{cases} \tag{15}$$

$$H_2^{v1}(x,y) = \begin{cases} H_A^{v1}(x,y) & \left|H_A^{v1}(x,y)\right| \geq \left|H_B^{v1}(x,y)\right| \\ H_B^{v1}(x,y) & \left|H_A^{v1}(x,y)\right| < \left|H_B^{v1}(x,y)\right| \end{cases} \tag{16}$$

$$H_2^{d1}(x,y) = \begin{cases} H_A^{d1}(x,y) & \left|H_A^{d1}(x,y)\right| \geq \left|H_B^{d1}(x,y)\right| \\ H_B^{d1}(x,y) & \left|H_A^{d1}(x,y)\right| < \left|H_B^{d1}(x,y)\right| \end{cases} \tag{17}$$

$$H_2^{h2}(x,y) = \begin{cases} H_A^{h2}(x,y) & \left|H_A^{h2}(x,y)\right| \geq \left|H_B^{h2}(x,y)\right| \\ H_B^{h2}(x,y) & \left|H_A^{h2}(x,y)\right| < \left|H_B^{h2}(x,y)\right| \end{cases} \tag{18}$$

$$H_2^{v2}(x,y) = \begin{cases} H_A^{v2}(x,y) & \left|H_A^{v2}(x,y)\right| \geq \left|H_B^{v2}(x,y)\right| \\ H_B^{v2}(x,y) & \left|H_A^{v2}(x,y)\right| < \left|H_B^{v2}(x,y)\right| \end{cases} \tag{19}$$

$$H_2^{d2}(x,y) = \begin{cases} H_A^{d2}(x,y) & \left|H_A^{d2}(x,y)\right| \geq \left|H_B^{d2}(x,y)\right| \\ H_B^{d2}(x,y) & \left|H_A^{d2}(x,y)\right| < \left|H_B^{d2}(x,y)\right| \end{cases} \tag{20}$$

The inverse wavelet transform will be taken to the resulting low and high frequency coefficients, we will get the fusion result of the second stage.

(3) The third stage: The fusion results of the first and second stage will be fused together. Suppose the two images are image F_1 **Error! Reference source not found.** and image F_2 **Error! Reference source not found.**.

Definition 2: The two images to be fused are image F_1 and image F_2. After the wavelet decomposition, the low frequency component of image F_1 is $L_{F1}(x,y)$ and the low frequency component of image F_2 is $L_{F2}(x,y)$. The high frequency component are represented by $H_{F1}^{h1}(x,y)$, $H_{F1}^{v1}(x,y)$, $H_{F1}^{d1}(x,y)$, $H_{F1}^{h2}(x,y)$, $H_{F1}^{v2}(x,y)$, $H_{F1}^{d2}(x,y)$,

$H_{F2}^{h1}(x,y)$, $H_{F2}^{v1}(x,y)$, $H_{F2}^{d1}(x,y)$, $H_{F2}^{h2}(x,y)$, $H_{F2}^{v2}(x,y)$, $H_{F2}^{d2}(x,y)$, they are the horizontal, vertical and diagonal high frequency components of the first and the second level, respectively.

The description is as follows:

a. the calculation method of the low frequency component

The proposed method here is similar to that of the first stage. It is still determined by calculating the regional energy of the low frequency coefficients, the energy formula is slightly different here. Suppose E_{F1} and E_{F2} represent the regional energy of the image F_1 and image F_2. The energy formulae are shown in (21) and (22) [15] [16].

$$E_{F1} = \sum_{x=1}^{3}\sum_{y=1}^{3} L_{F1}^2(x, y)\log L_{F1}^2(x, y) \tag{21}$$

$$E_{F2} = \sum_{x=1}^{3}\sum_{y=1}^{3} L_{F2}^2(x, y)\log L_{F2}^2(x, y) \tag{22}$$

Suppose the final low frequency component is $L(x, y)$ **Error! Reference source not found.**, the fusion formula of the low frequency component is shown in (23) [16].

$$L(x, y) = \begin{cases} L_{F1}(x, y) & E_{F1} \geq E_{F2} \\ L_{F2}(x, y) & E_{F1} < E_{F2} \end{cases} \tag{23}$$

b. the calculation method of the high frequency components

The high frequency component contains the detail information of an image. The regional standard deviation of images can reflect this. The larger the standard deviation, the more details it contains. The high frequency components of the two images are divided into discrete 3×3 regions. The formula for calculating the regional standard deviation is shown in (24) [21].

$$SD = \sqrt{\frac{1}{m\times n}\sum_{x=1}^{m}\sum_{y=1}^{n}(H(x,y)-\overline{H})^2} \tag{24}$$

$H(x,y)$ represents the high frequency component, $\overline{H}$ represents the mean value of the 3×3 region, $m=n=3$.

Suppose $H^{h1}(x,y)$, $H^{v1}(x,y)$, $H^{d1}(x,y)$, $H^{h2}(x,y)$, $H^{v2}(x,y)$, $H^{d2}(x,y)$ represent the first and second level fusion results of the horizontal, vertical and diagonal high frequency components, respectively. The fusion formulae are shown in (25)~(30).

$$H^{h1}(x, y) = \begin{cases} H_{F1}^{h1}(x, y) & SD_{F1}^{h1} \geq SD_{F2}^{h1} \\ H_{F2}^{h1}(x, y) & SD_{F1}^{h1} < SD_{F2}^{h1} \end{cases} \tag{25}$$

$$H^{v1}(x, y) = \begin{cases} H_{F1}^{v1}(x, y) & SD_{F1}^{v1} \geq SD_{F2}^{v1} \\ H_{F2}^{v1}(x, y) & SD_{F1}^{v1} < SD_{F2}^{v1} \end{cases} \tag{26}$$

$$H^{d1}(x, y) = \begin{cases} H_{F1}^{d1}(x, y) & SD_{F1}^{d1} \geq SD_{F2}^{d1} \\ H_{F2}^{d1}(x, y) & SD_{F1}^{d1} < SD_{F2}^{d1} \end{cases} \tag{27}$$

$$H^{h2}(x, y) = \begin{cases} H_{F1}^{h2}(x, y) & SD_{F1}^{h2} \geq SD_{F2}^{h2} \\ H_{F2}^{h2}(x, y) & SD_{F1}^{h2} < SD_{F2}^{h2} \end{cases} \tag{28}$$

$$H^{v2}(x, y) = \begin{cases} H_{F1}^{v2}(x, y) & SD_{F1}^{v2} \geq SD_{F2}^{v2} \\ H_{F2}^{v2}(x, y) & SD_{F1}^{v2} < SD_{F2}^{v2} \end{cases} \tag{29}$$

$$H^{d2}(x, y) = \begin{cases} H_{F1}^{d2}(x, y) & SD_{F1}^{d2} \geq SD_{F2}^{d2} \\ H_{F2}^{d2}(x, y) & SD_{F1}^{d2} < SD_{F2}^{d2} \end{cases} \tag{30}$$

The inverse wavelet transform will be taken to the resulting low and high frequency coefficients, we will get the final fusion result.

4. Experiments and Analysis

4.1. Evaluation Criteria

In order to evaluate the performance of the proposed method, we adopt the mean, information entropy (IE), standard deviation (SD) and average gradient (AG) as objective evaluation criteria to evaluate the results of our fusion method.

(1)The mean is the mean value of the image pixel values. It reflects the average brightness of an image. The calculation formula is shown in (31) [5].

$$\bar{I} = \frac{1}{m \times n} \sum_{x=1}^{m} \sum_{y=1}^{n} I(x, y) \tag{31}$$

$I(x, y)$ is the pixel value of an image, $m \times n$ is the size of an image.

(2)Information entropy is an important indicator of the evaluation of images. The calculation formula is shown in (32) [20].

$$H = -\sum_{i=0}^{L-1} P_i \log_2 P_i \tag{32}$$

P_i is the distribution probability of the gray value i, L is the total number of the gray level.

(3)Standard deviation reflects the image texture information. The larger the standard deviation, the more dispersed distribution of the gray levels of an image, the sharper textures. The calculation formula is shown in (33) [21].

$$SD = \sqrt{\frac{1}{m \times n} \sum_{x=1}^{m} \sum_{y=1}^{n} (I(x, y) - \bar{I})^2} \tag{33}$$

$I(x, y)$ is the pixel value of an image, $\bar{I}$ is the mean value of an image pixel values, $m \times n$ is the size of an image.

(4)Average gradient reflects the tiny details of variance, texture variation and image resolution. The greater the average gradient, the better the image resolution. The calculation formula is shown in (34) [20].

$$AG = \frac{1}{mn} \sum_{x=1}^{m} \sum_{y=1}^{n} \sqrt{\frac{[I(x+1, y) - I(x, y)]^2 + [I(x, y+1) - I(x, y)]^2}{2}} \tag{34}$$

$I(x, y)$ is the pixel value of an image, $m \times n$ is the size of an image.

4.2. Fusion Results

The method is experimented in MATLAB environment. The infrared and visible images in the experiment have been matched exactly, they were shot in the same scene and at the same time. Figure 3 shows a group of images in the experiment, figure 3(a) is an infrared image, figure 3(b) is a visible image. We can see a person in the infrared image, but we can't see the person in the visible image.


(a) Infrared image (b) Visible image


(c) Fusion result of AVE_MAX (d) Fusion result of the first stage


(e) Fusion result of the second stage (f) Fusion result of our method

Figure 3. Fusion Results

Figure 3(c) is the result of the simple fusion method AVE_MAX, figure 3(d) is the result of the first stage of our method, figure 3(e) is the result of the second stage of our method, figure 3(f) is the result of our method.

4.3. The Analysis

The fusion results are evaluated by the evaluation criteria mentioned in 4.1. The results are shown in table 1.

Table 1.The Evaluation of the Fusion Results

Method	the mean	IE	SD	AG
Figure3(c)	90.5426	6.3229	23.7689	7.4081
Figure3(d)	110.0739	6.8749	31.9445	8.2534
Figure3(e)	101.9224	6.6859	29.6004	8.7058
Figure3(f)	**110.0757**	**6.8912**	**32.2945**	**9.4266**

As can be seen from table 1, compared with the simple AVE_MAX fusion method, the performance of our method is much better. We obtain the final result by three stages of discrete wavelet transform, the final result is better than the results of the first two stages, especially the average gradient has more growth.

5. Conclusions

The wavelet transform fusion method can get good fusion result. In this paper, according to the characteristics of infrared and visible images, we have proposed a fusion method based on wavelet transform. We get the final fusion results through three stages of discrete wavelet transform. The results show that no matter from the perspective of the visual effect, or from the objective evaluation of fusion results, compared with the similar research methods, the results of our method are better, clearer. We have achieved more satisfactory results.

Acknowledgements

The authors would like to thank the anonymous reviewers and editors for their invaluable suggestions. The work was jointly supported by the National Natural Science of Foundation of China (NO. 61202351), Basic Science Research of Foundation of Nanjing University of Aeronautics and Astronautics (NO.2012133), China Postdoctoral Science Foundation (NO.2011M500124), General Program of University Natural Science of Jiangsu Province (NO.14KJD510004).

References

[1] G. Lei, L. Huihui and B. Yongsheng, “Editor, Image Fusion, Publishing House of Electronics Industry”, Bei jing, **(2008)**.
[2] C. Hao and W. Yanjie, “Study for Image Fusion Based on Wavelet Transform”, Microelectronics and Computer, vol. 5, no. 27, **(2010)**.
[3] W. Jian and Z. Shaofeng, “Visible and Infrared Image Fusion Method Based on Wavelet Transform and YUV”, Journal of Northwestern Polytechnical University, vol. 3, no. 33, **(2013)**.
[4] S. Yankui, Editor, “Wavelet Analysis and its Application”, China Machine Press, Beijing, **(2005)**.
[5] J. Zhuqing, “Study of Multi-Source Image Fusion Method in Transform Domain”, Ph D.Thesis, Jiangnan University, Wuxi, **(2011)**.
[6] M. Kumar and S. Dass, “A Total Variation-Based Algorithm for Pixel-Level Image Fusion”, IEEE Transactions on Image Procession, vol. 9, no. 18, **(2009)**.
[7] P.J. Burt, Editors, “A Gradient Pyramid Basis for Pattern Selective Image Fusion”, Processings of the Society for Information Display Conference, California, USA, **(1992)**, PP. 467-470.
[8] D.R. Barron and O.D.J. Thomas, “Image fusion though consideration of Texture Components”, IEEE Transactions on Electronics Letters, vol. 12, no. 37, **(2001)**.
[9] S.G. Mallat, “A theory for Multi-Resolution Signal Decomposition the Wavelet Representation”, IEEE Transactions on Pattern Analysis and Machine Intelligence, vol. 7, no. 11, **(1989)**.
[10] H.W. Chang and S.D. Lan, “Editors. Image Fusion Based On Addition of Wavelet Coefficients. International Conference on Wavelet Analysis and Pattern Recognition, Beijing, China, **(2007)**, pp. 1585-1588.
[11] H. Li, B.S. Manjunath and S.K. Mitra, “Multisensor image Fusion Using the Wavelet Transform”, Graphical Models and Image Processing, vol. 3, no.27, **(1995)**.

[12] L.J. Chipman and T.M. Orr, Editors, "Wavelets and Images Fusion", Proceedings of IEEE International Conference on Image Processing, Washington D. C., USA, **(1994)**, pp. 248-251.
[13] R. Sanjit, H. Tamanna, S.M. Mahbubur Rahman, "Image fusion Technique Using Multivariate Statistical Model for Wavelet Coefficients", Signal, Image and Video Processing, vol. 2, no. 7, **(2013)**.
[14] L. Fan, Y. Zhang, Z. Zhou, D.P. Semanek, S. Wang, and L. Wu, "An Improved Image Fusion Algorithm Based on Wavelet Decomposition", Journal of Convergence Information Technology, vol. 10, no. 5, **(2010)**.
[15] J. John, Lewis, J. Robert, O'Callaghan, "Pixel- and region-based image fusion with complex wavelets", Information Fusion, vol. 2, no. 8, **(2007)**.
[16] N. Yifeng, "Airborne Infrared and Visible Image Fusion for Target Perception Based on Target Region Segmentation and Discrete Wavelet Transform", Mathematical Problems in Engineering, vol. 10, no.22, **(2012)**.
[17] N. Kingsbury, "The Dual-Tree Complex Wavelet Transform: A New Technique for Shift Invariance and Directional Filters", Proceedings of 8th IEEE Digital Signal Processing, vol.8, no. 86, **(1998)**.
[18] J. Tian and L. Chen, "Adaptive Multi-Focus Image Fusion Using a Wavelet-Based Statistical Sharpness Measure, Signal Process, vol. 92, no.9, **(2012)**.
[19] R. Singh and A. Khare, "Fusion of Multimodal Medical Images Using Daubechies complex Wavelet Transform – A Multi Resolution Approach", Information Fusion, vol.19, no.49, **(2014)**.
[20] J. Li, J. Sun and X. Mao, "Multi Resolution Fusion of Remote Sensing Images Based on Resolution Degradation Model", Geo-Spatial Information Science, vol.1, no.8, **(2005)**.
[21] G. Piella, "New Quality Measures for Image Fusion", Proceedings of International Conference on Information Fusion, Stockholm, Sweden, **(2004)**, pp. 542-546.

Authors

Lingchao Zhan received the M.S. degree in Computer Application Technology from Shanghai Normal University in 2007. She is currently pursuing the Ph.D. degree in Computer Application Technology at Nanjing University of Aeronautics and Astronautics. Her current research interests include Image Processing. She is currently a lecturer in Nanhang Jincheng College.

Yi Zhuang is currently a professor and Doctoral tutor in College of Computer Science and Technology, Nanjing University of Aeronautics and Astronautics. Her current research interests include Information Security, Distributed computing, Image Processing, Network.

